第48卷 第2期
2010年4月

古脊椎动物学报
VERTEBRATA PALASIATICA

pp.119-132
figs.1-5

内蒙古中部新发现的始施氏貘(哺乳纲,奇蹄目)头骨材料[1)]

李 萍[1,2] 王元青[1*]

(1 中国科学院古脊椎动物与古人类研究所,脊椎动物进化系统学重点实验室 北京 100044 *通讯作者)
(2 中国科学院研究生院 北京 100039)

摘要:记述了产自内蒙古呼和勃尔和剖面阿山头组的始施氏貘(*Schlosseria magister*)幼年头骨、头骨碎片及产自额尔登敖包底白层的 *S. magister* 成年头骨。幼年头骨在脊齿貘科属首次描述,成年头骨材料也是目前 *S. magister* 中首次描述。幼年头骨主要特征如下:头骨细长,脑颅部略有扩张,有眶后突,眶后收缩明显,矢状脊轻微发育;鼻切迹浅,位于前臼齿列之前,由前颌骨和鼻骨构成;眼眶大,眶前缘位于 M1 后部上方,眶下孔位于 DP3-4 之上;基蝶骨向后向中央逐渐加厚,末端隆起;翼蝶骨很大,从腹面看向后向背侧扩展,末端形成三角形的翼蝶骨突,覆盖在卵圆孔上;岩骨岬部表面有内颈动脉及其分支留下的 3 条沟痕;最内侧的为内颈动脉内侧沟,沿着岬部弯曲前行至最前部;镫骨动脉沟短小,横跨在圆窗前腹侧;岬动脉沟最长,起始于卵圆窗前内侧,沿岬部向前延伸;弓形下窝所在位置平滑,无凹陷。*S. magister* 乳颊齿主要特征如下:DP2 冠面大致呈三角形,前窄后宽,前缘较尖,长明显大于宽;外脊上仅有一个中央主尖前尖,一个非常不明显的小棱(可能为雏形的原脊)紧贴在前尖后舌侧壁上;前、后附尖不明显。DP3 冠面呈梯形,与 DP2 相比明显增大,亚臼齿化,前附尖和后附尖略大,原、后脊明显。前尖大,后尖尚未分离;原尖很弱,几乎无法辨认,原脊低且不发育;次尖大而钝,比原尖更靠舌侧,后脊比原脊略发育,中部具小的后小尖;后脊在次尖处拐向后唇侧,使得磨蚀面呈 V 形。DP4 冠面近方形,完全臼齿化,后尖已从外脊上分化出来,比前尖稍小,向舌侧倾斜,后尖肋明显;舌侧尖、脊发育完好,原尖和次尖大而钝,原脊、后脊近乎平行,比 DP3 的更高更长;两条脊分别在原尖和后尖处拐向后唇侧方,形成 V 形的磨蚀面。

S. magister 在由幼年向成年转变的过程中,主要变化趋势如下:1) 吻部特征不同,主要表现为鼻切迹的位置、形态以及与之相关的前颌骨、上颌骨形态的差异。幼年头骨的鼻切迹位于前臼齿列之前,由前颌骨和鼻骨组成;成年头骨的鼻切迹后缩至 M1-2 之上,由鼻骨和上颌骨组成,并且因鼻切迹后缩造成鼻骨不与前颌骨接触。幼年和成年个体上颌骨的整体形态,眶前窝、眶下孔的位置和形态都差异显著。2) 与咀嚼功能相关的结构改变。幼年个体的矢状脊微弱,而成年个体的则高且突起,暗示了后者具有相对强大的颞肌,以适应咀嚼功能。对比发现,*S. magister* 与 *Lophialetes expeditus* 成年头骨在大小、整体形态和一些具有分类意义的特征上(如鼻骨和泪骨、前颌骨的接触方式,眶后突、关节后突、下颌关节窝的形状,矢状脊的高度等)非常接近。参照童永生、雷奕振(1984)对脊齿貘类头骨的划分方法,将 *Schlosseria magister* 的头骨与 *L. expeditus* 的划为一组,同时纠正了原有划分方案中存在的问题。

1) 国家自然科学基金重点项目(编号:40532010)、国家重点基础研究发展规划项目(编号:2006CB806400)、国家基础科学人才培养基金特殊学科点项目(编号:J0930007)和中国科学院化石发掘与修理专项基金资助。

收稿日期:2009-06-08

关键词:内蒙古二连盆地,始新世,脊齿貘科,头骨,乳齿
中图法分类号:Q915.873 **文献标识码**:A **文章编号**:1000-3118(2010)02-0119-14

NEWLY DISCOVERED *SCHLOSSERIA MAGISTER* (LOPHIALETIDAE, PERISSODACTYLA, MAMMALIA) SKULLS FROM CENTRAL NEI MONGOL, CHINA

LI Ping[1,2] WANG Yuan-Qing[1*]
(1 *Key Laboratory of Evolutionary Systematics of Vertebrates, Institute of Vertebrate Paleontology and Paleoanthropology, Chinese Academy of Sciences* Beijing 100044 * corresponding author: wangyuanqing@ivpp.ac.cn)
(2 *Graduate University of the Chinese Academy of Sciences* Beijing 100039 ruru0925@163.com)

Abstract Juvenile skull and skull fragment, together with an adult skull of *Schlosseria magister*, discovered in Nei Mongol, are described in this paper. The juvenile skull comes from the Arshanto Formation, Huheboerhe section, and represents the first known lophialetid juvenile skull. The adult specimen was discovered in the basal white layer of Erden (Urtyn) Obo, and is the first adult skull of *Schlosseria magister* ever described. The major differences between the juvenile and adult *S. magister* skulls lie in the contact of certain bones, the shape of the rostrum, and in some features related to masticatory function. Overall, adult *S. magister* and *Lophialetes expeditus* exhibit only minor differences in cranial characteristics. Problems in the classification of lophialetid skulls are also discussed in this paper.
Key words Erlian Basin, Nei Mongol; Eocene; Lophialetidae; skull; deciduous teeth

Schlosseria magister was erected by Matthew and Granger in 1926, based on a partial left maxilla with P1-M3, a right dentary with i2-3, c, and p4-m3, and fore and hind feet. Although its teeth are more primitive in morphology than those of *Lophialetes expeditus* (Matthew and Granger, 1925), their close resemblance led the authors (Matthew and Granger, 1926:3) to the conclusion that the teeth of *Lophialetes* are "directly derivable from those of *Schlosseria*". Furthermore, in spite of their rhino-like upper molars, both genera were assigned to the new subfamily Lophialetinae within the family Lophiodontidae. Since then, questions regarding their systematic position have been raised by different authors (e.g. Simpson, 1945; Gromova, 1952; Viret, 1958). This dispute finally ended when Radinsky (1965a) stated that "*Schlosseria* and *Lophialetes* appear to represent an independent line of Asiatic Eocene tapiroids" and raised Lophialetinae to family rank, since "they are equally distinct from lophiodontids and helaletids, and even more different from isectolophids". This view was accepted and widely cited by later researchers (e.g., Zhou and Qi, 1982; Tong and Lei, 1984; Dashzeveg and Hooker, 1997).

Lophialetidae is widely distributed in the Eocene sediments of Asia. Most of the Chinese specimens have been excavated in Nei Mongol (e.g., Matthew and Granger, 1925, 1926; Radinsky, 1965a; Ye, 1983; Qi, 1987). Lophialetids have also been reported from Henan (Tong and Lei, 1984; Wang and Zhou, 1982; Xu et al., 1979), Hubei (Cheng and Ma, 1990), Shandong (Zhou and Qi, 1982), Shanxi (Huang and Wang, 2001), Shaanxi (Zhang and Qi, 1981), Xinjiang (Zheng, 1978; Jin, 2000), and Yunnan (Huang and Qi, 1982; Zong et al., 1996; Huang, 1999). Outside of China there have also been a few reports, from Mongolia (Dashzeveg and Hooker, 1997), Kazakhstan (Biryukov, 1974; Lucas et al., 1997) and India (Ranga Rao, 1972; Sahni and Khare, 1972). Despite this wide distribution, no juvenile lophialetid skulls have ever been described. Recently, a juvenile and an adult skull of *Schlosseria magister* were collected from the Erlian Basin of central Nei Mongol, allowing us to describe the deciduous dentition of this species for the first time and draw some inferences about its cranial ontogeny.

Terminology of tooth description follows that of Hooker (1989), and the Chinese term follows translation of Zhou et al. (1975). Abbreviation: IVPP, Institute of Vertebrate Paleontology

and Paleoanthropology, Chinese Academy of Sciences.

1 Systematic description

Perissodactyla Owen, 1848
Ceratomorpha Wood, 1937
Tapiromorpha Haeckel, 1866
Tapiroidea Gray, 1825
Lophialetidae Radinsky, 1965
***Schlosseria* Matthew & Granger, 1926**
***Schlosseria magister* Matthew & Granger, 1926**
(Figs. 1–5)

Referred specimens IVPP V 16390, a relatively well preserved juvenile skull; IVPP V 16391, posterior part of a juvenile skull; IVPP V 16573, right half of an adult skull.

Localities and horizons V 16390, V 16391 were collected from the lower part of the Arshanto Formation, Huheboerhe, Erlian Basin, Nei Mongol (Inner Mongolia); Lower Eocene (Meng et al., 2007; Sun et al., 2009). V 16573 was collected from the basal white beds at Erden Obo. The basal white beds were thought to be Middle Eocene in age (Qi, 1990), but our recent investigations suggest that this needs to be reconsidered.

Description The preserved length of the juvenile skull V 16390 (Figs. 1, 2) is 110.8 mm. The nasals, premaxilla, zygomatic arches, frontals, parietals and occipitals are all damaged, and the right orbit and temporal fossa are heavily distorted. Regarding the dentition, the incisors and canines are lost; right DP3–4 are broken labially; the paracone of right M1 is broken; left DP2 is broken anteriorly; and M3 is in eruption on both sides. DP2–M1 are moderately worn and M2 is only slightly worn.

Dorsal view (Fig. 1A): the nasals are not preserved except the caudal ends. Judging from the impressions left by the nasals on matrix infilling the nasal cavity, the intact bones were probably long and thin, and probably extended rostrally from a position dorsal to M1 to beyond the diastema. The caudal ends of the bones expand laterally, touching the facial lachrymal expansion. The nasal-frontal suture is obscured by crushing; most likely the contact is transverse, with the frontals intruding between the nasals (Holbrook, 2001). The frontal is slightly concave between the well-developed supraorbital crests. Most of it is missing, exposing frontal crests that come together at an angle of 10° and converge caudally into a weak sagittal crest.

Lateral view (Fig. 2A–C): the maxilla is relatively long and deep, forming the main part of the face. The infraorbital foramen is large, extending from above the posterior part of DP3 to above the anterior part of DP4, and is level with the center of the orbit. About 6 mm above this foramen, a slender depression representing a deformed preorbital fossa exists on either side of the skull, although the fossa is deeper on the right due to taphonomic distortion. The position of the nasal incision is unclear, but it is unlikely to be above the premolars or molars, because at the level of these teeth the maxilla is high and, the part of the skull above them and below the nasal is filled with matrix, leaving no space for the nasal incision. Thus, it is possible that the nasal incision is very shallow and lies rostral to the premolars. The orbit is large and round, about 16 mm in diameter, with the anterior rim lying above the posterior part of M1. The maxillary tubercle bears M2–3 and forms a massive, thick orbital floor. Inside the orbit, the large facial foramen penetrates the maxilla and connects rostrally with the infraorbital foramen. The lachrymal lies on the rostrodorsal rim of the orbit and has an obvious triangular facial expansion that separates the frontal from the maxilla. The lachrymal borders the frontal dorsally, the maxilla and the jugal ventrally, and the palatine caudally. The lachrymal tubercle cannot be observed on this specimen because of damage to the anterior orbital rim. The jugal forms the

anteroventral border of the orbit and forms a broad contact with the maxilla rostrally, extending upward to contact the lachrymal. The sphenopalatine foramen lies in the middle of the orbit, at the mediolateral level of the long axis of M3. An obvious depression extending caudally from this foramen is present on each side. The depression on the right side is distorted and overhung by a thick and strong ridge. In life, this depression joins the sphenopalatine foramen with the orbital fissure, and marks the attachment of the external pterygoid muscle. The postorbital process is broken, leaving a weak and slender fragment. The parietal extends ventro rostrally into the heavily crushed temporal fossa and contacts the alisphenoid, precluding any squamosal-frontal contact. Inside the temporal fossa, there are several foramina associated with the sphenoid complex. The optic foramen is located on the orbitosphenoid, and two adjacent foramina lie caudoventral to it. The anterior one is the orbital fissure or anterior lacerate foramen, lying on the border of the orbitosphenoid and alisphenoid. The posterior one is the round foramen; it opens on the alisphenoid and is fused with the anterior opening of the alisphenoid canal.

Ventral view (Fig. 1B): the rostrally tapering palatine process of the maxilla is long and slightly concave in the middle. The palatine-maxilla suture lies at the level of the contact between DP4 and M1. Anterior palatine foramina are not evident in this specimen. At the level of the hypocone of M1, a pair of posterior palatine foramina is present. The internal nares open at a position just caudal to the level of M2. The vomer is very long; it extends from the position of the internal naris onto the bulging basisphenoid. It is slightly lower than the vertical plate of the palatine and remains at the same level along its entire length. The presphenoid is relatively narrow and long, and lies just anterior to the caudally and medially bulging basisphenoid. The posterior outline of the bulge is rectangular. The large alisphenoid forms the ventral wall of the temporal fossa, and in ventral view its most striking feature is its large and laterally expanded smooth surface. Medially, it ascends caudally and ramifies into two convex branches at a position medial to the posterior opening of the alisphenoid canal. The inner branch is inclined at 15° from the sagittal plane of the skull, and terminates at the opening of the middle lacerate foramen. The lateral branch is inclined at 30° from the inner one and thickens caudally, terminating in a triangular process (the alisphenoid tubercle) that overlaps the oval foramen ventrally. A deep groove separates this process from the postglenoid process. The squamosal is damaged and distorted on the right side, and on the left side only a short part of the zygomatic arch is preserved. Dorsally, the squamosal touches the parietal, but the suture is obscured. It seems that the suture is not exposed on the dorsal facet of the skull because of the broad lateral extension of the parietal. The glenoid fossa is flat in all directions and bounded caudally by the postglenoid process. The anterior surface of the process is almost vertical, whereas the posterior surface is inclined posteriorly at approximately 30° to the vertical plane and bears a shallow groove on its dorsal portion. At the dorsal end of this groove lies the postglenoid foramen.

Dentition: the teeth are damaged on both sides, but overall the two sides provide complementary information on the DP2–M3 cheek dentition (for measurements see Table 1).

Anterior to the right DP2, there is a diastema about 3 mm long, but it is unclear whether DP1 exists.

DP2 is sub-triangular in occlusal view and wider posteriorly than anteriorly, with a sharp anterior edge. The paracone is the only cusp on the ectoloph. It is anteroposteriorly elongated, and more convex labially than lingually. A tiny crista (incipient protoloph?) lies on its lingual side. The parastyle and metastyle are weak. The labial cingulum is well developed and almost continuous, being interrupted only at the base of the paracone. The lingual cingulum curves posteriorly from the base of the paracone to the metastyle, forming a shallow basin together with the ectoloph.

DP3 is much larger than DP2. Its anterior width is only about 2/3 of its posterior width, giving it a trapezoidal outline. Compared to DP2, it is submolarized with a distinct protoloph

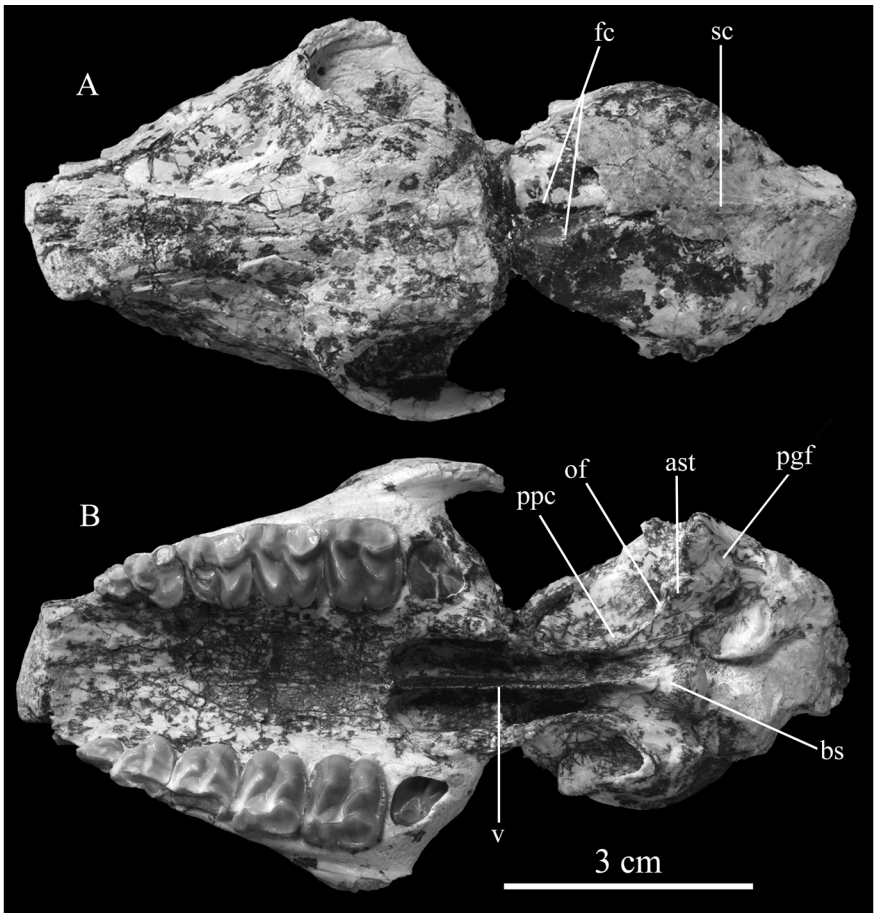

Fig. 1　*Schlosseria magister* juvenile skull (IVPP V 16390)
A. dorsal view; B. ventral view
Abbreviations: ast. alisphenoid tubercle 翼蝶骨突; bs. basisphenoid 基蝶骨; fc. frontal crest 额脊; of. oval foramen 卵圆孔; pgf. postglenoid foramen 关节后孔; ppc. posterior pterygoid canal 后翼管; v. vomer 犁骨; sc. sagittal crest 矢状脊

and metaloph, and a larger parastyle and metastyle. With moderate wear, the parastyle is only half the height of the paracone, and is well separated from the paracone by a clear notch on the labial side. The paracone is large, convex on both the labial and lingual sides, and appears cylindrical in labial view. The metacone is not isolated from the ectoloph. The protocone is faint and indistinct. The protoloph is low and weak; it extends forward from the protocone, being almost parallel to the ectoloph in its first half, and then turns about 90° to merge with the preparacrista. The hypocone is much larger, and more lingually located than the protocone; it is almost as high as the parastyle. The metaloph is also low, but better developed than the protoloph; it starts from the obtuse hypocone and extends vertically to join the ectoloph at the centrocrista with a small metaconule midway. Owing to wear, the hypocone becomes elongated towards the labial-posterior border of the tooth, forming a V-shaped wear facet on the metaloph. The basal cingulum is obvious and almost continuous in all directions, with only slight interruptions at the bases of the hypocone and paracone.

DP4 is fully molarized, with a well individualized metacone on the ectoloph, and well developed lingual cusps and lophs. As in DP3, the parastyle is distinct, the paracone is large,

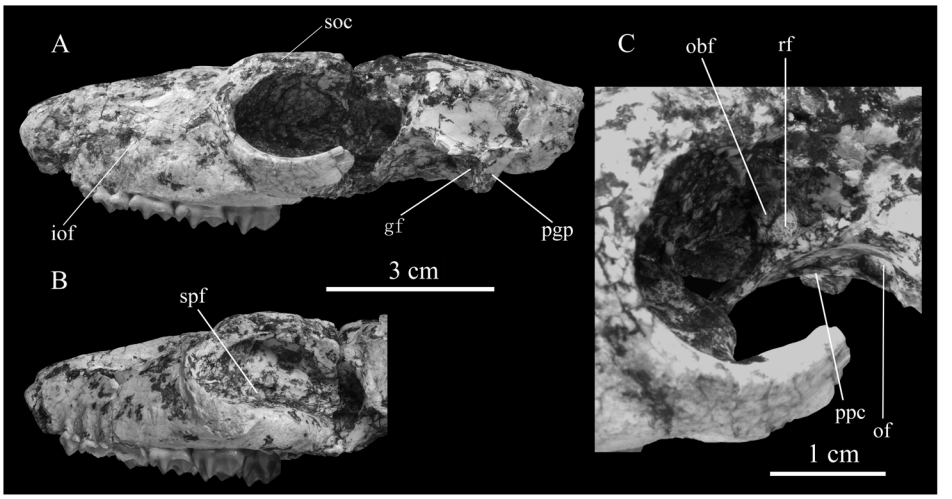

Fig. 2 *Schlosseria magister* juvenile skull (IVPP V 16390)
A. left lateral view; B. anterior view of right side (reversed); C. temporal fossa
Abbreviations: gf. glenoid fossa 下颌关节窝; iof. infraorbital foramen 眶下孔; obf. orbital fissure 眶蝶裂; of. oval foramen 卵圆孔; pgp. postglenoid process 关节后突; ppc. posterior pterygoid canal 后翼管; rf. round foramen 圆孔; soc. supraorbital crest 眶上脊; spf. sphenopalatine foramen 蝶腭孔

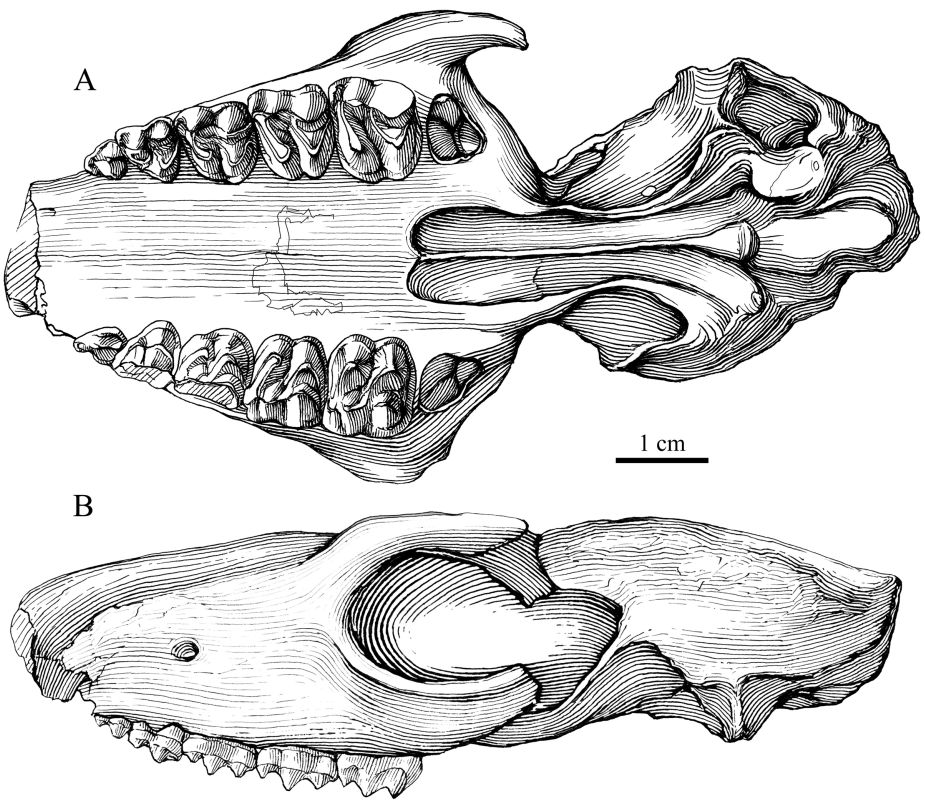

Fig. 3 Illustration of *Schlosseria magister* juvenile skull (IVPP V 16390)
A. ventral view; B. lateral view (left side)

and the basal cingulum is well developed on the labial, lingual, anterior and posterior sides; the labial cingulum is interrupted at the base of the paracone. However, DP4 is larger and is approximately square. Also, a tiny nodule lies in the valley between the protoloph and the metaloph on DP4. The metacone is slightly smaller than the paracone, is lingually deflected, and has a strong rib on the labial side. The protocone and hypocone are large and obtuse. The protoloph and metaloph are longer and higher than in DP3, oriented obliquely at a small angle to the transverse axis of the tooth but parallel to each other. Owing to wear, each of these lophs shows a V-shaped wear facet as in DP3.

M1 and M2 are rectangular, slightly wider than long, and similar to each other in morphology, differing only in that the latter is larger. Their cusps are higher, and their lophs longer, than in DP4. The metacone rib is weaker than in DP4. The protoloph and metaloph do not have V-shaped wear facets as in DP4. The basal cingulum is more developed anteriorly, posteriorly and labially than in DP4. The lingual cingulum is interrupted at the bases of both the hypocone and the protocone. As in DP4, both teeth have tiny nodules in the valley between the two lingual cusps.

M3 is still in eruption. From what can be observed, the development of the cusps and lophs is similar to the pattern in M1 and M2, but the posterior part is reduced due to a more lingually situated metacone.

Each tooth from DP4 to M3 has a prominent crista on the lingual slope of the paracone.

Table 1　Measurements of *Schlosseria magister* (V 16390) cheek teeth　(mm)

	Length	Width	L/W
right DP2	5.69	4.56	1.25
left DP3	7.32	7.82	0.94
left DP4	8.92	9.75	0.91
left M1	9.60	10.66	0.90
left M2	10.06	11.60	0.87
right M2	10.08	11.73	0.86
right DP2–M2		40.63	

V 16391 (Fig. 4A, A1; B, B1): only the caudal part of the frontal, the lateral side of the temporal, and parts of the parietal, sphenoid and petrosal are preserved.

Viewed dorsally, the frontal intrudes into the parietal at 45° to the longitudinal axis of the skull, approximately 5 mm behind the conspicuous postorbital constriction. The postorbital process is large and reaches into the orbit, terminating 5 mm over the presphenoid. Viewed ventrally, the alisphenoid is crushed, and there is no evidence for a caudolateral expansion and alisphenoid tubercle as in V 16390. Nevertheless, a pair of nutrient foramina does exist on the basisphenoid, a feature not observed in V 16390. The squamosal-alisphenoid suture can be seen between the alisphenoid process and the postglenoid process. The right petrosal of V 16391 is exposed. It is relatively well preserved, only slightly broken at its rostral and caudal ends, and partially covered by the distorted squamosal on the squamosal side.

The tympanic side of the petrosal faces ventrolaterally, and is marked by the almond-shaped promontorium cochlea. On the posterior edge of the promontorium are two obvious apertures. The larger, caudal one is the cochlear fenestra, which is closed by the secondary tympanic membrane in life. The rostrolateral one is the vestibular fenestra, which in life is closed by the footplate of the stapes. Immediately lateral to the vestibular fenestra and caudal to the co-

chlear fenestra, the stapedial fossa is present but deformed. The promontorium also bears three distinct grooves for the branches of the internal carotid artery. The medial ramus of the internal carotid artery is long, curving rostrally along the rim of the promontorium from the medial side of the cochlear fenestra. The stapedial artery sulcus is rather short and wide, lying anteroventrally across the vestibular fenestra. The promontory artery sulcus starts in front of the vestibular fenestra and runs along the lateral edge of the promontorium, ending at the rostral end of the promontorium.

Viewed from the cerebellar side, the subarcuate fossa is almost flat. Rostroventral to it is the internal acoustic meatus, which is divided into two deep pits by a strong transverse crista. The dorsal pit is the foramen for the vestibular ramus of the acoustic nerve, and is small and oblate. The ventral foramen is larger and rounder, and accommodates the cochlear ramus of the acoustic nerve.

The rostral end of the squamosal side of the petrosal is wrapped by the squamosal, so that the facial canal and the sulcus for the facial nerve cannot be observed. The posterior facet is an irregular but smooth surface.

Adult skull V 16573 (Fig. 5A, B): the preserved length of this skull is 183.2 mm. The occipital and the zygomatic arch of the temporal are lost; the orbit and the temporal fossa are not preserved.

This skull bears some similarities to that of *Lophialetes expeditus* (for details see 2.2),

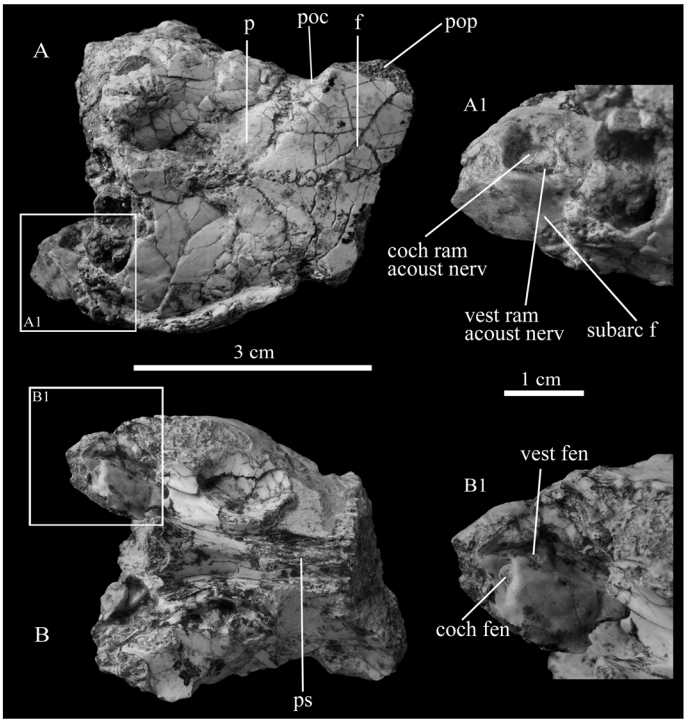

Fig. 4 Posterior part of a *Schlosseria magister* juvenile skull (IVPP V 16391)
A, A1. dorsal view; B, B1. ventral view
Abbreviations: coch fen. cochlear fenestra 蜗窗; coch ram acoust nerv. cochlear ramus of acoustic nerve 听神经耳蜗分支; f. frontal 额骨; p. parietal 顶骨; poc. postorbital constriction 眶后收缩; pop. postorbital process 眶后突; ps. presphenoid 前蝶骨; subarc f. subarcuate fossa 弓形下窝; vest fen. vestibular fenestra 前庭窗; vest ram acoust nerv. vestibular ramus of acoustic nerve 听神经前庭分支

which prevented an unambiguous assignment to *Schlosseria magister* on initial observation. However, the relatively low metaloph and the large and obtuse hypocone suggest that the teeth are probably not high-crowned, in contrast to that of *L. expeditus*. Additionally, the estimated premolar to molar length ratio is over 70%. Thus, we assign the skull to the genus *Schlosseria*, and refer it to the type species *S. magister*.

Dorsal view (Fig. 5A): the outline of the skull is slender. Most of the nasal is lost, leaving only the caudal end and the lateral expansion, which is broken above M2. The nasal-frontal suture cannot be detected. The postorbital process is large. The frontal crests are well developed and converge into a high sagittal crest. The jugal extends caudally almost without any lateral expansion.

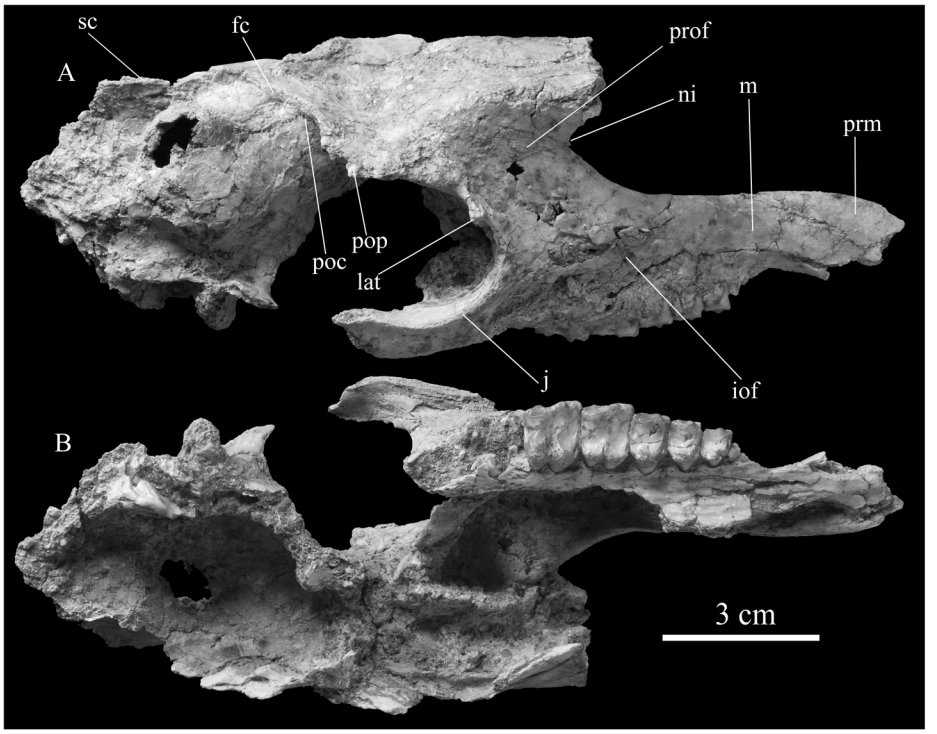

Fig. 5　Right half of a *Schlosseria magister* adult skull (IVPP V 16573)
A. dorsal and right lateral view; B. ventral view
Abbreviations: fc. frontal crest 额脊; iof. infraorbital foramen 眶下孔; j. jugal 颧骨; lat. lachrymal tubercle 泪结节; m. maxilla 上颌骨; ni. nasal incision 鼻切迹; poc. postorbital constriction 眶后收缩; pop. postorbital process 眶后突; prm. premaxilla 前颌骨; prof. preorbital fossa 眶前窝; sc. sagittal crest 矢状脊

Lateral view (Fig. 5A): the skull is high and elongated. The premaxilla is short; it overlies the foremost portion of the maxilla rostrally and ends caudally above the paracone of P1. The premaxilla-maxilla suture is straight, and its rostral end lies between the alveolus of I3 and the large canine. Separated by the nasal incision which is formed by the nasal and the maxilla, the maxilla is slender and low at the front, and then rises sharply to touch the lateral side of the nasal. The nasal-maxilla suture terminates over M1–2, and the nasal incision is retracted to the same point. The pronounced preorbital fossa lies behind the nasal incision, below the nasal, and rostral to the orbit. The infraorbital foramen is small, lying above the rostral edge of M1 and at the dorsoventral level of the middle of the orbit. The orbit is oval, and its margin is formed by the frontal, lachrymal and jugal. Its anterior rim lies over the middle of M3. The or-

bital floor is narrow and rather small in area. The lachrymal lies between the frontal and the maxilla; it is small and lacks an obvious facial expansion, indicating an absence of nasal-lachrymal contact. The lachrymal tubercle is triangular, protruding at the anterior rim of the orbit. The maxillary portion of the zygomatic arch extends back to the level of the posterior part of M2. The jugal touches the lachrymal at the level of the center of the orbit. The zygomatic arch of the temporal is broken at the root. The parietal is moderately expanded in its central area, and touches the temporal about one third of the way down the lateral side of the skull. Due to bad preservation, the contacts among the parietal, frontal and temporal are indiscernible.

Ventral view (Fig. 5B): the anterior facet of the glenoid fossa is partly broken. It is flat, lying almost perpendicular to the sagittal plane, and deepens at the squamosal root of the zygomatic arch, forming a deep and laterally extended broad groove. Caudally, it is bounded by a medium-sized postglenoid process that bears a distorted broad groove on its posterior facet. The postglenoid foramen is indiscernible. The tympanic bulla has been broken away, exposing the petrosal. The *crus commune*, the inner acoustic meatus and the two branches for the acoustic nerves can be observed in dorsal view. In ventral view, the short and thin medial ramus of the internal carotid artery can be seen to extend rostrally from a position about 2 mm anterior to the large cochlear fenestra.

Dentition: the teeth are heavily worn. P1 has two roots; the protocone of P2 and the parastyle of P3 are broken; M3 is broken away, leaving only the alveolus; the premolars have protoloph-metaloph loops. The estimated ratio of P1–4 length to M1–3 length is over 70%. The parastyle, paracone and metacone become increasingly larger from P2 to M2. Judging from the ectoloph, the crown is not high. Viewed on the moderately worn M2, the metaloph is low and the hypocone is large and obtuse.

2 Comparison and discussion

2.1 Comparison between juvenile and adult skulls of *Schlosseria magister*

Comparisons between juvenile and adult *S. magister* skulls indicate that the main changes in skull structure from juvenile to adult are the following. Firstly, modifications of the rostrum. In the juvenile skull, the nasal incision is formed by the premaxilla and nasal, and terminates anterior to the premolars. In the adult, the incision is formed by the maxilla and nasal, and consequently is retracted to a point above M1–2, precluding contact between the nasal and the premaxilla. Adults and juveniles also differ greatly in the shape of the maxilla, and in the shapes and positions of the preorbital fossa and infraorbital foramen (see description). Secondly, morphological changes related to masticatory function. In the adult skull, the sagittal crest is higher and much stronger, indicating that the temporal muscle was stronger and capable of producing higher masticatory forces.

The newly discovered juvenile and adult skulls of *S. magister* also provide important new information on the anatomy of this group. First, Radinsky (1965a) stated that, in both juvenile and adult skulls, the infraorbital foramen is located more rostrally in *S. magister* than in *L. expeditus*, suggesting that the former taxon has a shallower nasal incision. However, our specimens indicate that the nasal incision and infraorbital foramen lie rostral to the premolars and above DP3–4 (rather than above DP2–3 as stated by Radinsky) respectively in the juvenile *S. magister* skull, whereas the same features are located above M1–2 and above the anterior part of M1 (rather than above P2–3 as stated by Radinsky) in adults. The corresponding features lie above DP4 and DP3 in the *L. expeditus* juvenile skull, and above M1 and P4 in the *L. expeditus* adult skull. Thus, new materials indicate that the position of nasal incision is more rostral in juveniles of *S. magister* than in juveniles of *L. expeditus*, whereas the situation in adults is reversed. We believe that the positions of the nasal incision and infraorbital foramen are related to

individual ontogenetic age, and cannot be simply compared across taxa without this consideration. Furthermore, the relationship between nasal incision length and the position of the infraorbital foramen is still unclear, prompting us to caution against judging the caudal extent of the nasal incision according to the position of the infraorbital foramen. Second, it is only in rare cases that the petrosal is preserved in the skull, so that the new material significantly enriches our knowledge of the tapiromorph petrosal. Previously, tapiromorph petrosal had been described only in *Heptodon posticus* (Radinsky, 1965b; Cifelli, 1982) and *Hesperaletes borineyi* (Colbert, 2006). The promontorium of the *Heptodon* petrosal is smooth, without any trace of grooves for arteries. Also, the *Heptodon* petrosal lacks a distinguishable fossa for the tensor tympani or stapedial muscles, which presumably share the same groove as the facial nerve. The former muscle would attach at the anterior end of the groove, lateral to the facial nerve, whereas the latter would attach at the posterior end, medial to the nerve (Radinsky, 1965b). The petrosals of both the adult and juvenile *S. magister* skulls have three grooves for arteries on the promontorium, and a separate stapedial fossa. That of adult *Hesperaletes* is even more complicated, possessing a superior petrosal sinus sulcus and sigmoid sinus sulcus (Colbert, 2006). In addition, there is no indication of a subarcuate fossa in adult *Hesperaletes*; nevertheless, the subarcuate fossa of *S. magister* is almost flat in juveniles but deep in adults. Third, the juvenile *S. magister* skull preserves some features never previously described in lophialetids, including the long vomer extending to the basisphenoid, the bulge on the basisphenoid, and the large alisphenoid with its triangular tubercle. This tubercle was first described and named in an isectolophid, *Karagalax mamikhelensis* (Maas et al., 2001). In both juvenile *S. magister* and adult *K. mamikhelensis*, this tubercle is anteromedial to the postglenoid process and posterior to the oval foramen, and is separated from the postglenoid process by a groove.

2.2 Comparison between the skulls of adult *S. magister* and other lophialetids

At present, only three relatively complete lophialetid skulls have been described: those of *Eoletes gracilis* (Biryukov, 1974; Lucas et al., 1997), *Lophialetes expeditus* (Reshetov, 1975), and *Simplaletes xianensis* (Zhang and Qi, 1981). Descriptions of fragmentary skulls of cf. *Breviodon acares* and *Schlosseria hetaoyuanensis* have also been provided by Radinsky (1965a) and Tong and Lei (1984), respectively. Here, we will make a comparison between the adult *S. magister* skull and the skulls of other described lophialetids.

The adult skulls of *S. magister* and *L. expeditus* (Reshetov, 1975) are not easily distinguishable on the basis of size, general shape, or straightforward diagnostic characters such as the relationships of the nasal with the lachrymal and premaxilla, the shapes of the postglenoid process, postorbital process and glenoid fossa, and the degree of development of the sagittal crest. The differences are limited to the following relatively subtle ones: the premaxilla of *S. magister* ends caudally above P1 while that of *L. expeditus* ends above P2, and the lachrymal tubercle of the former is triangular while that of the latter is trapezoidal. In addition, the position of the infraorbital foramen differs between the two taxa, but this difference may be related to individual ontogenetic age.

Compared to *S. hetaoyuanensis* (Tong and Lei, 1984), the nasal incision of *S. magister* is greatly retracted. Both have a short diastema between I3 and the canine, and a long post-canine diastema. In *S. hetaoyuanensis*, the latter diastema is about as long as P1–2, whereas in *S. magister* it is 1.5 times as long as P1–2.

Radinsky (1965a) briefly compared *Breviodon* and *L. expeditus*. Due to the extensive similarities between *L. expeditus* and *S. magister* skulls, this comparison can also be applied to *S. magister*. *S. magister* and *Breviodon* skulls share some similarities at least in the caudal part of the skull. Both have a conspicuous postorbital constriction, moderately expanded braincase, and high and sharp sagittal crest. However, the former is much larger than the latter; and the

infraorbital foramen of *S. magister* lies above the anterior part of M1, whereas that of *Breviodon* lies above the posterior part of P2. In Radinsky's (1965a) description, *Breviodon* has a sharp keel on its basisphenoid, whereas the basisphenoid of *S. magister* bears a rounded bulge.

S. magister and *Simplaletes xianensis* (Zhang and Qi, 1981) are similar in the presence of a preorbital fossa, large orbit, triangular lachrymal tubercle, jugal-lachrymal contact, large postorbital process and conspicuous postorbital constriction. However, the skull of *S. magister* is slightly higher and obviously longer than that of *Sim. xianensis*; its dorsal surface is flat, with the nasal and frontal at the same level, while that of *Sim. xianensis* gradually ascends in the rostrocaudal direction. Also, the postorbital constriction of *S. magister* intrudes rostroventrally under the large postorbital process, forming an inclined surface, while that of *Sim. xianensis* forms a vertical groove. The premaxilla of both skulls are short, but in *Sim. xianensis* the premaxilla ascends sharply to touch the nasal and form a shallower nasal incision situated above the canine. Furthermore, the pocket-like preorbital fossa of *Sim. xianensis* is deeper and broader, stretching from the anterior orbital rim to above P1; the orbital floor is also much larger in this taxon than in *S. magister*.

The following features occur in both *S. magister* and *Eoletes gracilis* (Biryukov, 1974; Lucas et al., 1997): rostrum long, with low anterior portion; preorbital fossa present; large postorbital process; and well developed sagittal crest. However, the nasal incision of *Eoletes gracilis* is much shallower, lying over the canine, and its premaxilla contacts the nasal. The infraorbital foramen of *S. magister* lies rostral to the preorbital fossa, whereas that of *E. gracilis* lies inside the preorbital fossa. Due to poor preservation, it is impossible to determine whether or not the postorbital process of *S. magister* extends ventrally, whereas that of *E. gracilis* extends ventrally and almost touches the zygomatic arch. Furthermore, *E. gracilis* has a relatively smaller orbit whose rostral rim is situated further rostrally, lying above M1–2; its sagittal crest is also relatively weaker than that of *S. magister*.

Radinsky (1965b) pointed out that, throughout the evolution of tapirs, one very important trend affecting the morphology of the skull has been retraction of the nasal incision. Tong and Lei (1984) later used rostral traits to classify Asian lophialetid skulls into three types, conforming to categories established by Radinsky: the first group is composed of *Eoletes gracilis* and *Simplaletes xianensis*, which are similar to *Heptodon* (nasal incision very shallow, above the canine; nasal long, nasal-premaxilla suture short, nasal-maxilla suture long; preorbital fossa absent); the second group includes *Lophialetes expeditus*, which is similar to *Colodon* (nasal incision very deep, retracted to a point above M2; nasal short, nasal-maxilla suture short, nasal does not contact premaxilla; preorbital fossa deep); and the third, intermediate group contains *Schlosseria hetaoyuanensis* (nasal incision moderately retracted; nasal contacts premaxilla; preorbital fossa shallow). Due to some misinterpretations of certain features, as discussed below, this classification is problematic and not very convincing. First, according to a restudy of *Eoletes gracilis* (Lucas et al., 1997), this species in fact possesses a shallow, anteroposteriorly elongated preorbital fossa. Our observations have indicated that the preorbital fossa of *Simplaletes xianensis* is very deep and broad. Thus, absence of the preorbital fossa should not be considered as a common feature of the first group. Additionally, Radinsky (1965b) stated that the nasal incision was above P1 and above the post-canine diastema (closer to P1 than to the canine) in *Heptodon calciculus* and *Heptodon posticus* respectively. However, that of *E. gracilis* and *Sim. xianensis* are shallower than that of *Heptodon*, being situated above the canine. Therefore, it is reasonable to assign the skulls of *E. gracilis* and *Sim. xianensis* to one group, but their skulls should not be classified with that of *Heptodon*. If we follow the classification of Tong and Lei (1984), *Schlosseria magister* should be assigned to the second group based on its cranial morphology. Nevertheless, it should be noted that the rostrum of *S. hetaoyuanensis* is very poorly preserved, so that the position of its nasal incision cannot be determined with certainty. It may

be over the post-canine diastema as the authors suggested, but could also lie more posteriorly. Thus, even though *S. hetaoyuanensis* has a high ascending premaxilla that stands in contrast to the low and short premaxilla of *S. magister* and *L. expeditus*, we do not exclude the possibility that its skull should be assigned to the same group as those of *S. magister* and *L. expeditus*. More detailed discussion of this issue will only be possible following further discoveries of better preserved materials.

Acknowledgements Li Chuankui, Meng Jin, Ni Xijun, Zhou Wei, Jin Xun, Li Qian, Bai Bin, Cao Qiang, Li Qiang, Chen Wei, Li Shijie, and Li Qi from the IVPP, Sun Chengkai from Shandong Provincial Museum, K. Christopher Beard from the Carnegie Museum of Natural History and Daniel L. Gebo from the Northern Illinois University participated in field work. Critical comments from Li Chuankui and Zhang Zhaoqun helped to improve this paper. Tong Yongsheng and Olivier Maridet helped in finding some publications. Corwin S. Sullivan, Olivier Maridet and Zhijie Jack Tseng helped to improve the English manuscript. Meng Jin kindly provided casts of specimens kept in the AMNH, and Liu Zhongyun provided access to the specimens in the IVPP collections. Photographs were taken by Gao Wei, drawings were made by Shen Wenlong. Particular thanks are given to Xie Shuhua and Li Qi for their patience and exquisite skills in preparing the materials. This research was supported by the National Natural Science Foundation of China (Grant No. 40532010), the Major Basic Research Project of the Ministry of Science and Technology of China (Grant No. 2006CB806400), the National Fund for Talent Training in Basic Science (Grant No. J0930007) and the Special Fund for Fossil Excavation and Preparation of the Chinese Academy of Sciences.

References

Biryukov M D, 1974. New genus of the family Lophialetidae from the Eocene of Kazakhstan. In: Materials on the History of Fauna and Flora of Kazakhstan, vol. 6, The Fauna and Flora from Mesocainozoic of South Kazakhstan. Alma-Ata: Zoological Institute, Academy of Sciences of Kazakhstan SSR. 57–73(in Russian)

Cheng J(程捷), Ma A C(马安成), 1990. The new mammalian materials from the Eocene of Liguanqiao Basin. Vert PalAsiat (古脊椎动物学报), **28**(3): 228–244(in Chinese with English summary)

Cifelli R L, 1982. The petrosal structure of *Hyopsodus* with respect to that of some other ungulates, and its phylogenetic implications. J Paleont, **56**(3): 795–805

Colbert M W, 2006. *Hesperaletes* (Mammalia: Perissodactyla), a new tapiroid from the Middle Eocene of southern California. J Vert Paleont, **26**(3): 697–711

Dashzeveg D, Hooker J J, 1997. New ceratomorph perissodactyls (Mammalia) from the Middle and Late Eocene of Mongolia: their implications for phylogeny and dating. Zool J Linn Soc, **120**: 105–138

Gromova V, 1952. Primitive tapiroids from Paleogene of Mongolia. Tr Paleont Inst Akad Nauk SSSR, (41): 99–119(in Russia)

Holbrook L T, 2001. Comparative osteology of early Tertiary tapiromorphs (Mammalia, Perissodactyla). Zool J Linn Soc, **132**: 1–54

Hooker J J, 1989. Character polarities in early perissodactyls and their significance for *Hyracotherium* and infraordinal relationships. In: Prothero D R, Schoch R M eds. The Evolution of Perissodactyls. New York: Oxford University Press. 79–101

Huang X S, 1999. Middle Eocene mammals of Lijiang Basin, Yunnan. In: Wang Y Q, Deng T eds. Proceedings of the Seventh Annual Meeting of the Chinese Society of Vertebrate Paleontology. Beijing: China Ocean Press. 125–138

Huang X S(黄学诗), Qi T(齐陶), 1982. Notes on Late Eocene tapiroids from the Lunan Basin, eastern Yunnan. Vert PalAsiat (古脊椎动物学报), **20**(4): 315–326(in Chinese with English abstract)

Huang X S(黄学诗), Wang J W(王景文), 2001. New materials of tapiroid and rhinocerotoid remains (Mammlia, Perissodactyla) from the Middle Eocene of Yuanqu Basin, central China. Vert PalAsiat(古脊椎动物学报), **39**(3): 197–203(in Chinese with English abstract)

Jin H Y(金海月), 2000. Middle Eocene mammals of Jeminay, Xinjiang. Vert PalAsiat(古脊椎动物学报), **38**(2): 135-146 (in Chinese with English summary)

Lucas S G, Emry R J, Bayshashov B U, 1997. Eocene Perissodactyla from the Shinzhaly River, eastern Kazakhstan. J Vert Paleont, **17**: 235-246

Maas M C, Hussain S T, Leinders J J M et al., 2001. A new isectolophid tapiromorph (Perissodactyla, Mammalia) from the Early Eocene of Pakistan. J Paleont, **75**: 407-417

Matthew W D, Granger W, 1925. The smaller perissodactyls of the Irdin Manha Formation of Mongolia. Am Mus Novit, (199): 1-9

Matthew W D, Granger W, 1926. Two new perissodactyls from the Arshanto Eocene of Mongolia. Am Mus Novit, (208): 1-5

Meng J, Wang Y Q, Ni X J et al., 2007. New stratigraphic data from the Erlian Basin: implications for the division, correlation, and definition of Paleogene lithological units in Nei Mongol (Inner Mongolia). Am Mus Novit, (3570): 1-31

Qi T, 1987. The Middle Eocene Arshanto fauna (Mammalia) of Inner Mongolia. Ann Carnegie Mus, **56**: 1-73

Qi T(齐陶), 1990. A Paleogene section at Erden Obo, Nei Mongol and on the discovery of *Pastoralodon lacustris* (Pantodonta, Mammalia) in that area. Vert PalAsiat(古脊椎动物学报), **28**(1): 25-33(in Chinese with English summary)

Radinsky L B, 1965a. Early Tertiary Tapiroidea of Asia. Bull Am Mus Nat Hist, **129**: 183-214

Radinsky L B, 1965b. Evolution of the tapiroid skeleton from *Heptodon* to *Tapirus*. Bull Mus Comp Zool, **134**(3): 69-106

Ranga Rao A, 1972. New mammalian genera and species from the Kalakot zone of Himalayan foot hills near Kalakot, Jammu and Kashmir State, India. Directorate Geol Oil Nat Gas Comm Dehra Dun, India, Spec Pap, **1**: 1-22

Reshetov V Y, 1975. Review of the early Tertiary tapiroids of Mongolia and the USSR. Tr Sovmest Sov-Mong Paleont Eksped, **2**: 19-53(in Russian)

Sahni A, Khare S K, 1972. Additional Eocene mammals from the Subathu Formation of Jammu and Kashmir. J Palaeont Soc India, **17**: 31-49

Simpson G G, 1945. The principles of classification and a classification of mammals. Bull Am Mus Nat Hist, **85**: 1-350

Sun B(孙勃), Yue L P(岳乐平), Wang Y Q(王元青) et al., 2009. The magnetostratigraphy of early Paleogene strata of Erlian Basin. J Stratigr(地层学杂志), **33**(1): 62-68(in Chinese with English abstract)

Tong Y S(童永生), Lei Y Z(雷弈振), 1984. Fossil tapiroids from the Upper Eocene of Xichuan, Henan. Vert PalAsiat(古脊椎动物学报), **22**(4): 260-280(in Chinese with English summary)

Viret J, 1958. Perissodactyla. In: Priveteau J ed. Trait Paleont, **6**(2): 368-475

Wang B Y(王伴月), Zhou S Q(周世荃), 1982. Late Eocene mammals from Pingchangguan Basin, Henan. Vert PalAsiat(古脊椎动物学报), **20**(3): 203-215(in Chinese with English summary)

Xu Y X(徐余瑄), Yan D F(阎德发), Zhou S Q(周世荃) et al., 1979. Subdivision of the red beds of Li-Guan-Qiao Basin with description of fossil mammals therefrom. In: Inst Vert Paleont Paleoanthrop, Nanjing Inst Geol Palaeont eds. Mesozoic and Cenozoic Red Beds of South China. Beijing: Science Press. 416-432(in Chinese)

Ye J(叶捷), 1983. Mammalian fauna from the Late Eocene of Ulan Shireh area, Inner Mongolia. Vert PalAsiat(古脊椎动物学报), **21**(2): 109-117(in Chinese with English summary)

Zhang Y P(张玉萍), Qi T(齐陶), 1981. A new species of *Simplaletes* (Lophialetidae, Mammalia) from the lower Tertiary of Shaanxi Province. Vert PalAsiat(古脊椎动物学报), **19**(3): 214-217(in Chinese with English abstract)

Zheng J J(郑家坚), 1978. Mammalian fossils of Liankan Formation, Turfan Basin and its geologic age. Mem Inst Vert Paleont Paleoanthrop, Acad Sin(中国科学院古脊椎动物与古人类研究所甲种专刊), (13): 116-125(in Chinese)

Zhou M Z(周明镇), Qi T(齐陶), 1982. Mammals from the Middle Eocene Kuanchuang Formation of Xintai, Shandong. Vert PalAsiat(古脊椎动物学报), **20**(4): 302-313(in Chinese with English summary)

Zhou M Z(周明镇), Qiu Z X(邱占祥), Li C K(李传夔), 1975. Some suggestions for unifying translation of nomenclature of the primitive eutherian molar-teeth. Vert PalAsiat(古脊椎动物学报), **13**(4): 257-266(in Chinese)

Zong G F(宗冠福), Chen W Y(陈万勇), Huang X S(黄学诗) et al., 1996. Cenozoic Mammals and Environment of Hengduan Mountains Region. Beijing: China Ocean Press. 80-85(in Chinese with English summary)